

Contract No.:

This manuscript has been authored by Savannah River Nuclear Solutions (SRNS), LLC under Contract No. DE-AC09-08SR22470 with the U.S. Department of Energy (DOE) Office of Environmental Management (EM).

Disclaimer:

The United States Government retains and the publisher, by accepting this article for publication, acknowledges that the United States Government retains a non-exclusive, paid-up, irrevocable, worldwide license to publish or reproduce the published form of this work, or allow others to do so, for United States Government purposes.

Developing Radiation Tolerant Polymer Nanocomposites Using C₆₀ as an Additive

Jonathan H. Christian,^a Joseph A. Teprovich Jr.,^a Jason Wilson,^a James C. Nicholson,^a Thanh-Tam Truong,^a Matthew R. Kesterson,^a Josef A. Velten,^a Ingo Wiedenhöver,^b Lagy T. Baby,^b Maria Anastasiou,^b Nabin Rijal,^b and Aaron L. Washington II^{a,}*

a. Savannah River National Laboratory, Aiken, South Carolina, 29803, USA.

b. Department of Physics, Florida State University, Tallahassee, Florida, 32306, USA

Email: Aaron.Washington@srl.doe.gov

Keywords: radiological, polymers, thin films, modeling

Abstract

In nuclear facilities utilizing plutonium, polymeric materials are subjected to long-term, close-contact, and continuous α radiation exposure, which can lead to compounding material degradation and eventual failure. Herein we model the attenuation of α particles by linear-low-density polyethylene (LLDPE), polyvinyl alcohol (PVA) thin films, and C₆₀ using Monte Carlo N-Particle Extended (MCNPX) software. The degradation of these materials was then investigated experimentally by irradiating them with a beam of α particles of 5.8 MeV energy at a tandem Van-De-Graaff accelerator delivering a dose rate of 2.95×10^6 rad/sec over a 3 mm

sample area. PVA nanocomposites containing 5 wt % C₆₀ were found to withstand ~ 7 times the α dose of undoped PVA films before a puncture in the film was detected. When these films were adhered to a LLDPE sheet the dual layer polymer was capable of withstanding about 13 times the dose of LLDPE and nearly 2 times the dose of the doped PVA thin film alone, thus demonstrating that polymer layering provides synergistic resistance to α particle induced degradation. X-ray diffraction measurements confirm a breakdown in PE crystallinity following irradiation, which we propose is a mechanism of degradation in these materials. The results herein help to resolve a prevalent technical challenge faced in nuclear facilities that utilize polymeric materials for nuclear processing.

Introduction

Polymeric materials are susceptible to alteration by ionizing radiation. This alteration is of particular concern when a continuous dose is delivered to the material. Continuous exposure can lead to compounding material defects that result in a greater likelihood of material failure. Thus, while many commonly used polymeric materials are useful for short-term applications in radiological environments due to their low cost, durability, and impenetrability towards water, their inability to withstand alteration from long-term radiation exposure is undesirable.¹

In general, the extent of polymer alteration by ionizing radiation is dependent on the radiation source, the dose, and the type of polymer being irradiated. Therefore, the dissociation, abstraction, and addition reactions that often lead to alteration by cross-linking or chain scission, can occur on varying timescales after irradiation.^{1,2,3} Upon alteration, a slew of undesirable physical changes can occur such as polymer softening, decreased ductility, an increase or decrease in the melting temperature, and embrittlement.^{1,2} Despite the ubiquity of polymers and

SRNL-STI-2016-00365

the well-known radiation induced degradation they can experience, a small amount of work has been done to improve the performance of these materials in radiation environments. The majority of said work has been directed at remediating the effects of gamma radiation on these materials through the addition of “antirad” compounds to the polymer matrix.^{4,5,6,7} These antirads can decrease the reaction rates of chain scission and cross-linking by scavenging radicals, intermediates, and ejected electrons as they form during irradiation.⁴ For example, 2-vinylnaphthalene and 4-vinylbiphenyl have been used to increase γ radiation resistance of poly(vinyl chloride) (PVC)⁴, and aromatic diacetylenes have been shown to remediate radiation induced damage in polyurethane.⁸ In many applications, however, polymeric materials are frequently subjected to a variety of ionizing radiation types.

Alpha (α) radiation has been especially overlooked in terms of its material altering properties due to its low energies and high mass, which can be readily attenuated. However, long-term exposure to α radiation can still cause unwanted material alteration at material surfaces which can accumulate and lead to material failure. This was exemplified in March of 2002 when the Los Alamos National Laboratory (LANL) experienced an unexpected release of ²³⁸Pu due to failure of a polytetrafluoroethylene (PTFE) valve seal that was badly degraded from close exposure to α emissions.⁹ Incidentally, α -emitting plutonium waste is often stored in linear-low-density polyethylene (LLDPE) bags to prevent contamination while awaiting permanent disposal. In this interim state, LLDPE also undergoes rapid degradation especially when in close contact with α sources.¹⁰ This degradation can cause the bags to become brittle and susceptible to puncturing, which can result in radiological contamination to surrounding areas. To mitigate this risk, the current practice is to periodically repackage the waste in new LLDPE bags. The degraded bags then contribute negatively to the overall level of waste, leading to increased costs

SRNL-STI-2016-00365

for the disposing entity and increased risk of worker exposure. Furthermore, decomposition of the LLDPE hydrocarbon has the potential to generate hydrogen gas that can accumulate over time, creating a flammability and over-pressurization hazard in closed environments.¹⁰

While polymer durability and puncture resistance have improved in recent years through the use of various additives^{11,12} and metallocene catalysts^{13,14,15} commercial availability of radiation tolerant polymers remains scarce. Recently, polymer nanocomposites based on various forms of carbon (e.g. carbon black, carbon nanotubes, graphene) have been used for improved mechanical properties^{11,16,17,18} although to date, no work has been done to study the effects of α radiation on carbon-based nanocomposites. However, we postulate that the high electron density of these carbon materials is ideal for quenching the charge differential of α particles as they travel through a doped polymer. This quenching should limit the damage resulting from α particle/polymer interactions. To test this idea, we developed a Monte Carlo N-Particle Extended (MCNPX) model to simulate α particle interactions with carbon materials and various host polymers. Our computational results show that the penetration depth of incident α radiation through carbon materials is significantly lower than in the modelled polymers.

With this in mind, we experimentally studied for the first time, the effects of α radiation on polymer nanocomposites utilizing water soluble C₆₀. We report herein on the fabrication of these materials and the extended lifetime they experience with respect to α particle induced puncture. Radiation resistance was tested using a beam of 5.8 MeV α particles from a Tandem Van de Graaff accelerator, which was delivered over a 3 mm diameter onto a polymer surface. Our nanocomposites withstood nearly seven times the dose of an undoped PVA film, and over thirteen times the dose of a LLDPE sheet. This development of a more durable polymer radiological containment system through doping with an electron-dense additive provides a

quick and convenient method for improving existing polymer systems to achieve enhanced radiation resistance, and appears to be a fruitful new research area.

Experimental Section

Modeling

Monte Carlo N-Particle Extended (MCNPX) modeling software was used to determine α particle penetration depth through various solid state materials. In our model, a sphere of plutonium oxide, generating 5.8 MeV α particles, was surrounded by 60 μm of various materials of interest. The model split the surrounding material into 1 μm layers and simulated the path of the α particles as they penetrated through these layers. The number of α particles that passed through each successive layer were then tallied to determine the depth at which the particles were completely attenuated in the material.

A COMSOL Multiphysics 2D axisymmetric thermal model was also used to simulate the heating effects caused by irradiating LLDPE and PVA films, 100 mm in diameter by 150 μm thick, with 5.8 MeV of α particles with varying currents from 1 to 50 nA . The model was used to ensure that heating effects caused by irradiation were not significant enough to cause our samples to melt when tested with the accelerator beam, a result that would prevent us from observing the long-term radiological degradation effects imparted on the polymers by the α particles.

Synthesis

Water dispersible C_{60} was prepared according to modified literature methods.^{19,20} PVA with a molecular weight of 9,000 -10,000 g/mole and 80% hydrolyzed and C_{60} were purchased

SRNL-STI-2016-00365

from Sigma Aldrich. Metallocene catalyzed LLDPE sheets were purchased from Extra Packaging Corporation.

Thin film development

PVA thin films were made by slowly pouring 12 g of an aqueous PVA solution (10 wt. %) onto flat, 3 in. X 4 in. glass substrates. Doped films were made by adding water soluble C₆₀ to 12 g of an aqueous PVA solution (10 wt. %) followed by gentle stirring to ensure complete carbon dispersion. The mixture was then poured onto a glass substrate. All films were left undisturbed to dry for 24 hrs. Once dry, the films were peeled from the glass substrate to yield transparent, malleable, free-standing films. Pre-fabricated LLDPE radiological containment bags were coated by pouring our doped PVA mixture onto the bag substrate that was partitioned into 3 in. x 4 in. sections using tape. Once dry, the films were well adhered to the LLDPE.

Optical Microscopy

Thin film thickness was measured using an Olympus SZX16 optical microscope with an image acquisition system.

Accelerator Facility

A Super-FN tandem Van de Graaff accelerator located at the Florida State University John D. Fox laboratory was used to accelerate helium ions to a total energy of 5.8 MeV, delivered as twice positive ions. Under our operating conditions the accelerator delivered a 2.95×10^6 rad/sec dose rate of α particles over a 3 mm diameter.

X-ray Diffraction (XRD)

SRNL-STI-2016-00365

Single sheets of each studied polymer were measured using XRD to quantify crystallinity before and after irradiation. Data were collected on a Bruker D8 X-ray Diffractometer by step scanning over a 2θ range of 5-70° with a step size of 0.02° and a dwell time of 1 s. Search-match identification of all the phases was performed with Jade software (Version 2010) from Materials Data Inc. combined with the PDF-4 database from the International Centre for Diffraction Data.

Fourier Transform Infrared Spectroscopy (FTIR)

Single sheets of each studied polymer were measured using a ThermoNicolet Nexus 670 FTIR equipped with an Attenuated Total Reflectance (ATR) sampling unit. The spectral resolution of the instrument is nominally 2 cm^{-1} . Background scans were obtained prior to sample scanning and improvement in the signal to noise ratio was obtained by averaging multiple interferograms for sample spectra.

Results and Discussion

MCNPX Modeling

The model we developed to calculate the penetration depth of α particles through various materials was constructed with a sphere of PuO_2 surrounded by a solid state material, as shown in Figure 1. The packing density, molecule density, and electron density of the solid state layer could be programmed to match any material, but for this study, was constrained to LLDPE, PVA, and C_{60} . The specific density parameters for these materials are given in Table 1.

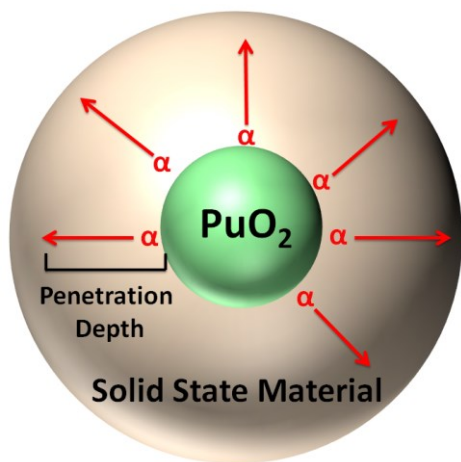


Figure 1. A 3D rendering of our α particle penetration model.

Table 1. Density data for the solid state materials in this study.

Solid State Material	Packing Density (g/cm ³)	Molecule Density (molecule/cm ³)	Electron Density (electrons/cm ³)
LLDPE	0.93	5.60×10^{20}	9.00×10^{21}
PVA	1.20	1.64×10^{22}	3.94×10^{23}
C_{60}	1.65	1.21×10^{21}	4.53×10^{23}

Our model simulated the particle physics (Coulombic and kinetic interactions) over the path of the α particles as they penetrated through 1 μm layers of the solid state material. The

distance at which the particles were completely attenuated is hereafter referred to as the penetration depth. Smaller penetration depths correlate to greater α attenuation. Materials with small penetration depths promise to enhance radiation resistance due to their ability to rapidly dissipate radiation energy, thus limiting material damage. In Figure 2, the collisions of α particles with each successive 1 μm layer in LLDPE, PVA, and C_{60} are shown. Our simulations determined that the penetration depth was 32 μm , 36 μm , and 41 μm for C_{60} , PVA, and LLDPE respectively. These depths correspond to a respective decrease in electron density for the materials, thus confirming increased attenuation is proportional to the electron density.

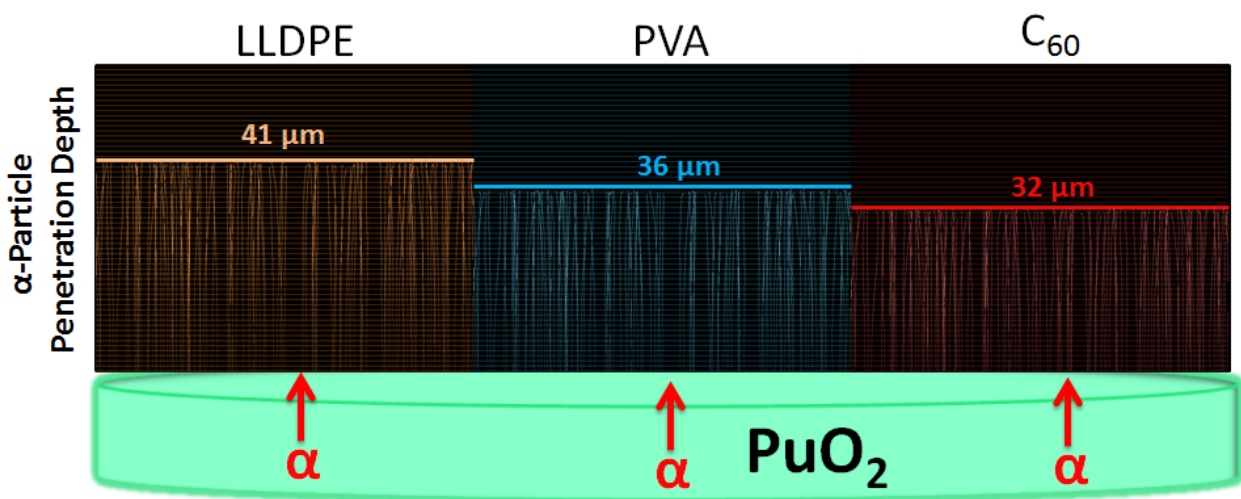


Figure 2. Simulated α -particle collisions in LLDPE, PVA, and C_{60} . The vertical colored lines represent α -particle collisions through each medium.

To determine the effects of on- and off-contact radiation exposure, we also simulated the α particle penetration through the thin films with no space present between the α particle source and the film (on-contact exposure), and with air gaps (off-contact exposure) of 100 μm , 3 mm, and 1 cm between the film and the radiation source. Because an α particle's penetration range in air is approximately 4.5 cm, off-contact exposure was utilized to test for air's attenuation effects.

Pragmatically, slightly off-contact is the expected form of material exposure in most real applications while on-contact exposure represents the worst case scenario for material irradiation. The probability of simulated α particle interactions in these films for on- and off-contact exposure is shown in Figure 3. The 100 μm air gap revealed only a small effect on decreasing the α penetration depth, while the 3 mm and 1 cm gaps caused a significant decrease in the penetration depth through the simulated materials. Our penetration depth simulations were used as a guide for thickness development of our radiation tolerant thin films. In order to ensure that no α particles exited the attenuating media, we developed films that were significantly thicker ($\sim 150 \mu\text{m}$) than the simulated penetration depths.

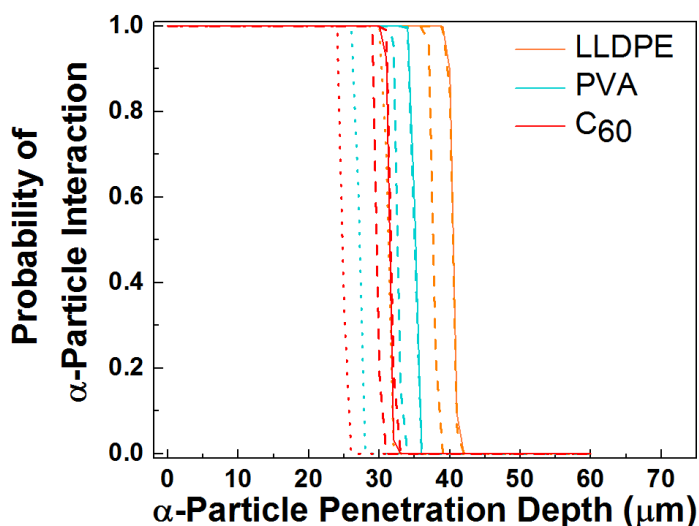


Figure 3. The simulated probability of α particle interactions with LLDPE, PVA, and C₆₀. The solid trace represents on-contact exposure while the dotted and dashed traces represent 3 mm and 1 cm air gaps respectively between the irradiated material and the radiation source. The 100 μm air gap data is omitted for clarity since it is nearly the same as the on-contact data.

To ensure the degradation of our films during accelerator tests (*vide supra*) was solely due to α radiation and not by melting from an overly intense beam, COMSOL Multiphysics was

SRNL-STI-2016-00365

used to simulate the temperature of LLDPE and PVA as a function of α beam diameter and beam current. The beam diameter was varied from 1 - 3 mm and the current from 1 – 50 nA. Our simulations represent a worst-case scenario from a thermal standpoint, as they assume that all of the energy of the α particles is added to the irradiated materials in the form of thermal energy. Additionally the energy of the modelled particles goes to zero, and the endothermic energy associated with removing electrons from the irradiated material was not considered. In actuality the α particles do not go to a zero energy state and some heat would be removed from ionization events. As can be seen in Figure 4, the temperature of both LLDPE and PVA increases with beam current and a smaller beam size causes greater heating of the polymer at lower currents. Using these simulations, we were able to optimize our accelerator test parameters to minimize heating effects on the studied polymers. Specifically, the accelerator current was fixed at 12 nA and the beam diameter was 3 mm. According to our worst-case scenario simulations, these parameters could only induce heating up to temperatures less than the melting/softening points of our polymer samples.

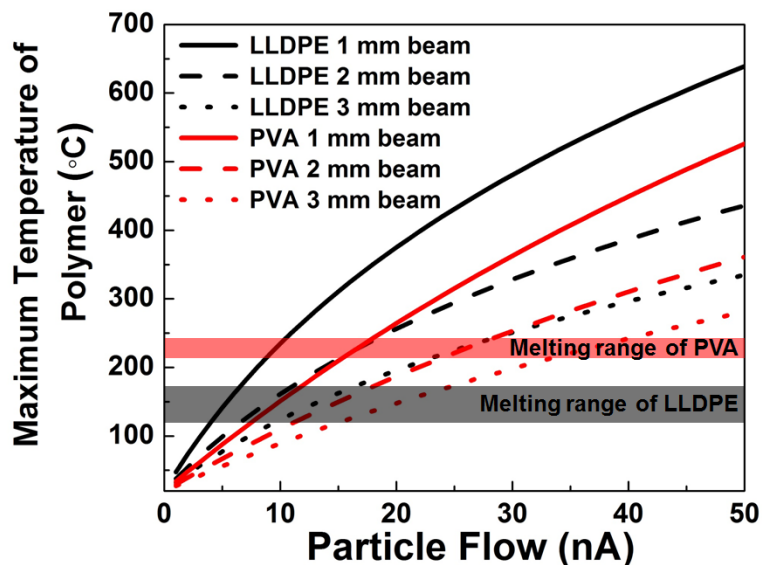


Figure 4. Steady state maximum temperatures of LLDPE and PVA as a function of α particle flow rate and beam diameter.

Thin Film Accelerator Tests.

Four types of samples were used for α particle exposure testing: a $150 \pm 10 \mu\text{m}$ thick sheet of “as purchased” LLDPE, a $150 \pm 10 \mu\text{m}$ thick PVA thin film with no additives, a $150 \pm 10 \mu\text{m}$ thick PVA thin film containing 5 wt. % C_{60} , and a $150 \pm 10 \mu\text{m}$ thick PVA thin film containing 5 wt. % C_{60} that was well adhered to a $150 \pm 10 \mu\text{m}$ thick sheet of as purchased LLDPE. PVA was chosen due its cost, availability, solubility, and transparency. These properties would allow for a commercializable platform that could easily retrofit existing polymer containment systems. Cross sectional microscopy images used to measure the thickness of each sample are shown in Figure 5.

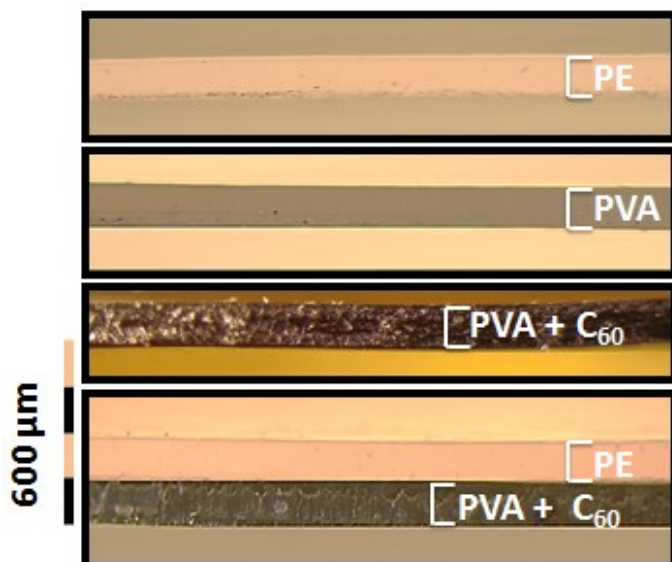


Figure 5 Optical microscopy images of polymer cross sections show that the thickness of each material is $150 \pm 10 \mu\text{m}$.

Following fabrication, each sample was exposed to 5.8 MeV accelerated charged helium nuclei (i.e. α particles) in a Van de Graaff accelerator employing a 2.95×10^6 rad/sec dose rate. This high dose rate was employed to accelerate the effects of ^{238}Pu α radiation that the polymers would experience over an extended period of time while being used for radiological containment. During exposure, a Faraday detector, placed 6 inches behind our irradiated samples, was used to detect when a breach occurred in the testing materials. A threshold current for the detector was fixed at 12 nA which we correspond directly to a puncture in the sample. This allowed us to accurately measure how long it took to penetrate the samples. The time spent in the beam could then be extrapolated to the time of on-contact ^{238}Pu exposure before material puncture. Following irradiation each sample was visibly altered as shown in Figure 6. In this figure, degradation and puncture in the films can be seen by observing the distortion in the background text and image. More visible degradation is apparent for the doped films due to the substantially longer exposure time they were able to withstand before being punctured.

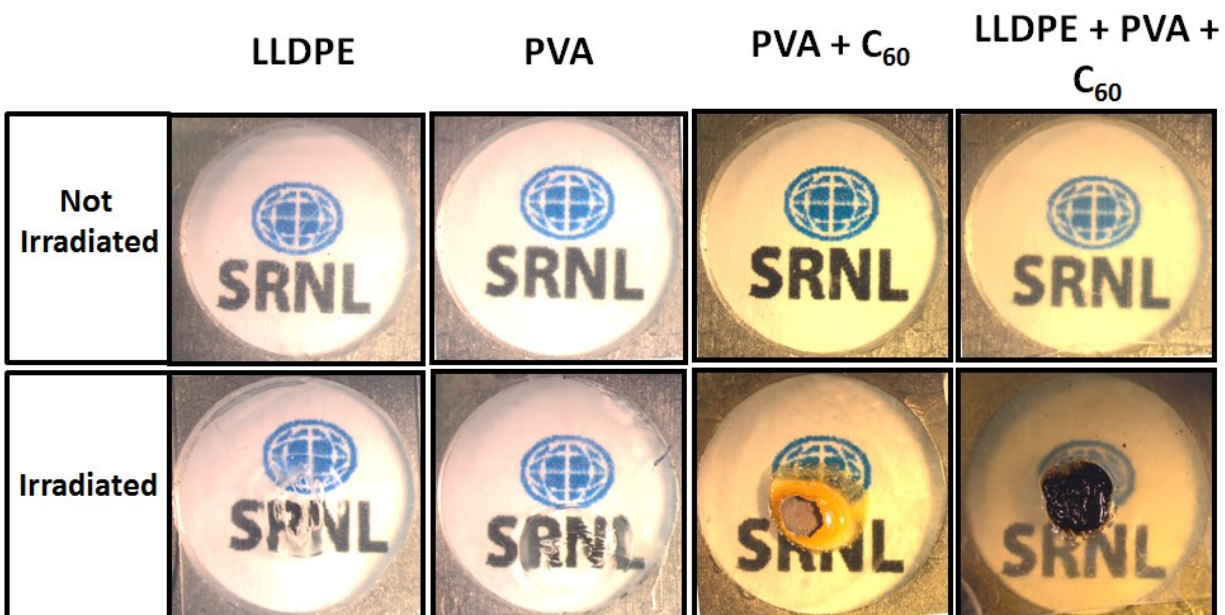


Figure 6. Each studied sample is shown before and after α irradiation. The background image is used to show sample transparency, color, and radiation damage induced to each polymer film.

After five measurements on each sample, we found that the average time for puncture in the LLDPE was 16.5 min. Undoped PVA thin films lasted only slightly longer and were punctured in 18.1 min. PVA thin films containing C₆₀ were punctured in 123.2 min, and the PVA thin film containing C₆₀ that was adhered to LLDPE was punctured in 217.5 min. These times correspond to irradiation dose rates of 2.92×10^9 rad/sec, 3.21×10^9 rad/sec, 2.18×10^{10} rad/sec, and 3.85×10^{10} rad/sec for LLDPE, undoped PVA, doped PVA, and doped PVA on a LLDPE substrate respectively. These data are summarized in Table 2.

Using the dose absorbed by our polymers and nanocomposites in the accelerator and the typical dose emitted by ²³⁸Pu metal ($\sim 5.88 \times 10^3$ rad/sec) over the same surface area as our accelerator samples (3 mm), the lifetime until puncture of each sample in a ²³⁸Pu environment was calculated. The puncture times in a ²³⁸Pu environment would be 5.8 days, 6.3 days, 42.9 days, and 75.8 days for LLDPE, undoped PVA, doped PVA, and doped PVA on a LLDPE

SRNL-STI-2016-00365

substrate respectively. Importantly, these times represent the worst-case performance of the studied materials, one in which the full dose from ^{238}Pu is absorbed through direct contact and only on a 3 mm target area. In actuality where on- and off-contact exposure occur, and the α dose is distributed among a larger surface area, the time until puncture would be considerably longer.

Our results show there is a strong correlation between the electron densities of each irradiated material and the resistance towards α -particle induced puncture, which is in excellent agreement with our modeling data. Additionally, some synergism appears to occur when coating the PVA film onto LLDPE as evidenced by the non-linear improvement in penetration resistance for the doped PVA on a LLDPE substrate in comparison to doped PVA and LLDPE alone. The time until puncture of our nanocomposites clearly show that C_{60} is an excellent additive for improving the resistance towards radiological-induced puncture in PVA.

Table 2. Irradiated material characteristics

Sample	Average Time to Puncture in Accelerator (min)	Average α-particle Dose Absorbed Before Puncture (rad/sec)	Estimated Time Until Puncture in a ^{238}Pu Environment (days)
LLDPE Sheet	16.5	2.92×10^9	5.8
PVA thin film with no additives	18.1	3.21×10^9	6.3
PVA thin film doped with C_{60}	123.2	2.18×10^{10}	42.9
PVA thin film doped with C_{60} and adhered to a sheet of LLDPE	217.5	3.85×10^{10}	75.8

To better understand the mechanism of degradation in our samples, we performed XRD and FTIR measurements on each sample pre- and post-irradiation. XRD measurements of pre-irradiated LLDPE (Figure 7) show that the material is highly crystalline with sharp diffraction

peaks corresponding to polyethylene. Several other peaks are present in the diffraction pattern and are tentatively ascribed to metallocene catalyst which is copolymerized with the olefin monomers during resin synthesis.²¹ Following irradiation, the LLDPE becomes noticeably more amorphous as evidenced by the formation of two broad humps in the diffraction pattern. We believe the breakdown of the LLDPE crystallinity is an important mechanism of degradation, as a highly crystalline LLDPE is more durable than its amorphous analogue.²² Further, the additional peaks attributed to metallocene are noticeably absent from post-irradiated samples, thus suggesting the large absorbing cross-section of metallocene^{14,15} makes it particularly prone towards radiation induced degradation.

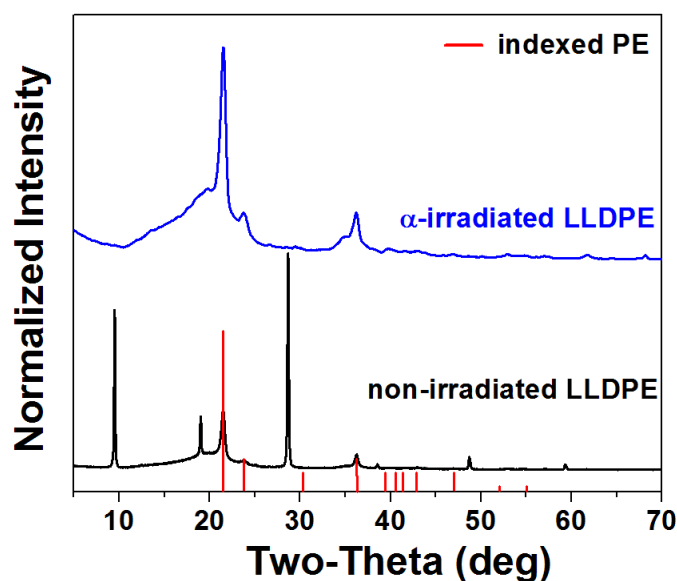


Figure 7. XRD measurements of pre- and post- α -irradiated LLDPE are shown with the diffraction pattern of polyethylene. The irradiated analogue becomes noticeably less crystalline following irradiation.

Measurements of undoped pre- and post-irradiated PVA films (Figure 8) show an amorphous structure in both cases due to retention of water resulting from our drop-casting

fabrication process. When C_{60} is added to the polymer matrix a sharp peak is seen at 26° . This peak corresponds to the most intense diffraction line from graphitic carbon, and confirms that C_{60} is well encapsulated in the films. The other diffraction peaks from graphitic carbon are not well-resolved presumably due to the low dopant concentration. It is also observed that the relative intensity of this peak to the amorphous hump between 10° - 25° is greater in the irradiated sample than it is in the unirradiated sample. This result suggests that as the PVA matrix breaks down and the intensity of its reflections diminish, the C_{60} dopant remains undamaged.

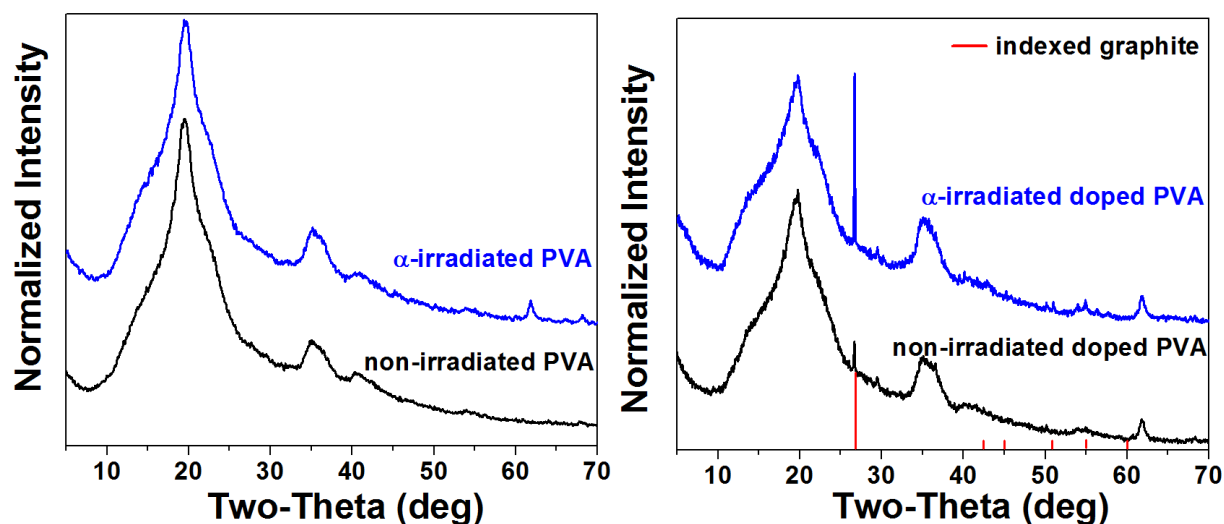


Figure 8. XRD measurements of a pre- and post- α -irradiated PVA thin film (left) and C_{60} -doped PVA thin film(right). Both films are amorphous as evidence by the broad humps in their diffraction patterns. The sharp peak at 26° in the doped pattern corresponds to the most intense diffraction line for graphitic carbon, a result that indicates C_{60} is encapsulated into the film.

FTIR spectra of pre and post-irradiated LLDPE and PVA films are shown in Supporting Information Figures 2, 3, and 4. Our measurements revealed that none of the studied polymers undergo functional group changes following irradiation. In fact, all LLDPE and PVA spectra

SRNL-STI-2016-00365

were in excellent agreement with their respective literature spectra.^{23,24} The spectra of doped PVA films were subtly different than undoped films, showing a small difference in the peaks $\sim 3000\text{ cm}^{-1}$, likely from the small amount of C_{60} dopant present.

Radiation Tolerant Bag Development

As stated at the onset of this manuscript, α -emitting plutonium waste is often stored in LLDPE bags to prevent contamination while awaiting permanent disposal; however, the LLDPE undergoes rapid degradation from the waste. To prove that our technique for generating enhanced polymers can be easily adapted to retrofit existing polymers, we drop casted a $150\text{ }\mu\text{m}$ thick layer of C_{60} doped PVA onto an existing LLDPE bag. Once dry, the coated LLDPE was folded into a bag shape and the edges were sealed using a low temperature plastic sealer. The resultant prototype (Figure 9) is a new radiological containment bag with enhanced resistance towards radiation puncture and degradation.



Figure 9. LLDPE radiological containment bag prototype coated with a PVA/ C_{60} thin film.

Conclusions

The effects of α radiation on polymer films and polymer nanocomposites utilizing C_{60} were studied. Our results show that the nanocomposite films exhibit exceptional resistance towards α radiation induced embrittlement and penetration compared to LLDPE and PVA. These results were in agreement with our MCNPX modeling of α attenuation through various media. These nanocomposites can be easily coated on existing polymer substrates in order to retrofit existing materials that are vulnerable towards degradation in nuclear environments. Further investigations and modeling of different polymer additives and various manufacturing techniques are currently underway to seek additional improvement of LLDPE and other polymers towards radiation induced degradation.

Associated Content

FTIR spectra of pre- and post-irradiated materials, and simulations of the probability of α particle interactions with PE, PVA, and C₆₀ with on-contact α exposure and 100 μ m, 3 mm, and 1 cm air gaps between the α source and the irradiated material are supplied in the Supporting Information.

Author Information

Corresponding Author

*E-mail: Aaron.Washington@srnl.doe.gov

Notes

The authors declare no competing financial interest.

Acknowledgements

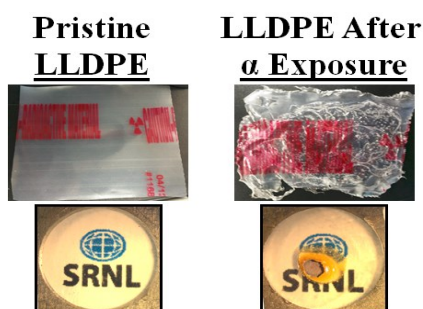
Work at SRNL was supported by the U.S. Department of Energy, Office of Deactivation & Decommissioning, and Facility Engineering (EM-13). The SRNL group thanks Stephen Hardee and Hope Hartman for assistance with thin film preparation.

References

1. Clough, R. L.; Shalaby, S. W., *Irradiation of Polymers: Fundamentals and Technological Applications*. 1st ed.; American Chemical Society, Washington, DC, **1996**.
2. Ivanov, V. S., *Radiation Chemistry of Polymers*. Khimiya-Leningrad, Russia: **1992**.
3. Skeins, W. E.; Williams, J. L., *Ionizing Radiation Effect on Selected Biomedical Polymers*. Society of Plastics Engineers. Chapter 44, pp. 1001-1018, **1987**.
4. Garcia-Uriostegui, L.; Dionisio, N.; Burillo, G., Evaluation of 2-Vinylnaphthalene and 4-Vinylbiphenyl as Antirads to Increase the Radiation Resistance of Poly(vinyl chloride). *Polym. Degrad. Stab.* **2013**, *98*, 1407-1412.
5. Zhang, X.; Pi, H.; Guo, S., Photostabilizing Efficiency of Ultraviolet Light Stabilizers for Rigid Poly(vinyl chloride) Against Photo-Oxidation. *Polym. Eng. Sci.* **2012**, *53* (2), 378-388.
6. da Silva, W. B.; Aquino, K. A. d. S.; de Vasconcelos, H. M.; Araujo, E. S., Influence of Copper Chloride and Potassium Iodide Mixture in Poly(vinyl chloride) Exposed to Gamma Irradiation. *Polym. Degrad. Stab.* **2013**, *98* (1), 241-245.
7. Wazzan, A. A.; Ismail, M. N.; Abd El Ghaffar, M. A., Evaluation of Some Polyaromatic Amines as Antirads and Antifatigue Agents in SBR Vulcanizates. *Int. J. Polym. Anal. Charact.* **2005**, *10* (1-2), 57-69.
8. Burillo, G.; Beristain, M. F.; Sanchez, E.; Ogawa, T., Effects of Aromatic Diacetylenes on Polyurethane Degradation by Gamma Irradiation. *Polym. Degrad. Stab.* **2013**, *98*, 1988-1992.
9. Fisher, G. L.; Lakis, R. E.; Davis, C. C.; Szakal, C.; Swadener, J. G.; Wetteland, C. J.; Winograd, N., Mechanical Properties and the Evolution of Matrix Molecules in PTFE Upon Irradiation with MeV Alpha Particles. *Appl. Surf. Sci.* **2006**, *253*, 1330-1342.

10. Reed, D. T.; Hoh, J.; Emery, J.; Okajima, S.; Krause, T., Gas Production Due to Alpha Particle Degradation of Polyethylene and Polyvinyl Chloride. *Office of Scientific and Technical Information* **1998**.
11. Kim, S.; Do, I.; Drzal, L. T., Thermal Stability and Dynamic Mechanical Behavior of Exfoliated Graphite Nanoplatelets-LLDPE Nanocomposites. *Polym. Compos.* **2010**, *31* (5), 755-761.
12. Singh, A., Irradiation of Polymer Blends Containing a Polyolefin. *Radiat. Phys. Chem.* **2001**, *60* (4-5), 453-459.
13. Starck, P., Dynamic Mechanical Thermal Analysis on Ziegler-Natta and Metallocene Type Ethylene Copolymers. *Eur. Polym. J.* **1997**, *33* (3), 339-348.
14. Neuse, E. W.; Rosenberg, H., Metallocene Polymers. *Journal of Macromolecular Science, Part C* **1970**, *4* (1), 1-145.
15. Togni, A.; Halterman, R. L.; (eds), *Metallocenes: Synthesis Reactivity Applications*. Wiley-VCH Verlag GmbH, Weinheim, Germany: 1998.
16. Huang, J. C., Carbon Black Filled Conducting Polymers and Polymer Blends. *Adv. Polym. Technol.* **2002**, *21*, 299-313.
17. Kim, H. J.; Abdala, A. A.; Macosko, C. W., Graphene/Polymer Nanocomposites. *Macromolecules* **2010**, *43*, 6515-6530.
18. Moniruzzaman, M.; Winey, K. I., Polymer Nanocomposites Containing Carbon Nanotubes. *Macromolecules* **2006**, *39*, 5194-5205.
19. Shane, D. T.; Corey, R. L.; Rayhel, L. H.; Wellons, M.; Teprovich, J. A.; Zidan, R.; Hwang, S.-J.; Bowman, R. C.; Conradi, M. S., NMR Study of LiBH₄ with C₆₀. *J. Phys. Chem. C* **2010**, *114* (46), 19862-19866.

20. Ward, P. A.; Teprovich, J. A.; Peters, B.; Wheeler, J.; Compton, R. N.; Zidan, R., Reversible Hydrogen Storage in a LiBH₄-C₆₀ Nanocomposite. *J. Phys. Chem. C* **2013**, *117* (44), 22569-22575.
21. Peacock, A. J., *Handbook of Polyethylene*. Marcel Dekker, Inc.: New York, NY, USA, 2000.
22. Piorkowska, E.; Rutledge, G. C., Eds, *Handbook of Polymer Crystallization*. John Wiley & Sons, Hoboken, NJ, USA: 2013.
23. Gulmine, J. V.; Janissek, P. R.; Heise, H. M.; Akcelrud, L., Polyethylene Characterization by FTIR. *Polym. Test.* **2002**, *21* (5), 557-563.
24. Mansur, H. S.; Sadahira, C. M.; Souza, A. N.; Mansur, A. A. P., FTIR Spectroscopy Characterization of Poly(vinyl alcohol) Hydrogel with Different Hydrolysis Degree and Chemically Crosslinked with Glutaraldehyde. *Mater. Sci. Eng., C* **2008**, *28* (4), 539-548.



Synopsis: The attenuation of alpha particles is modelled through various media using Monte-Carlo N-Particle Extended software. Using tandem Van-de-Graaff accelerator tests it is shown that the lifetime of polymers in alpha radiation environments can be significantly enhanced through doping with C₆₀ fullerenes.